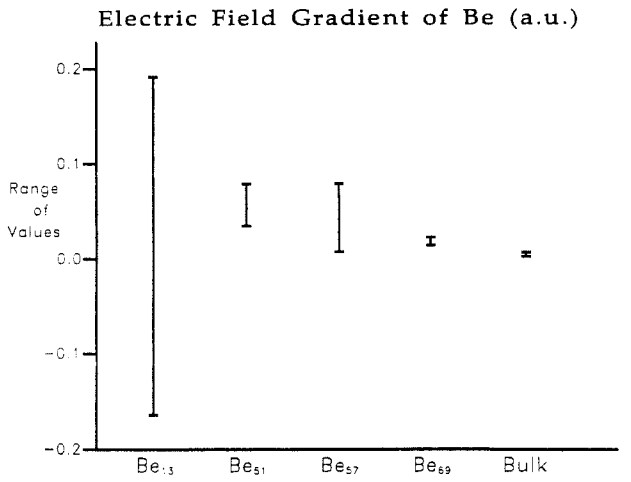

Figure 3. Range of values of electric field gradient ($3.241\,23 \times 10^{15}$ esu·cm^{-3}/au) for Be_{13}, Be_{51}, Be_{57}, Be_{69} and experiment as given in ref 8 (bulk value assumed to be positive).

size increases. As we proceed to clusters beyond Be_{69} in future studies, we may expect some oscillations in convergence patterns that depend on cluster shapes.

Acknowledgment. This research was partially supported by the National Science Foundation under Grants CHE-8214689 and CHE-8912674 and by a grant from Cray Research, Inc. The Ohio Supercomputer Center and the Pittsburgh Supercomputing Center are acknowledged for grants of supercomputer time. We thank Dr. Victor Luana for helpful discussions. This work was performed under the auspices of the Division of Material Sciences of the Office of Basic Energy Sciences, U.S. Department of Energy, and Lawrence Livermore National Laboratory under contract No. W-7405-Eng-8.

Appendix

The group theoretical arguments for approximating the reduction in the number of integrals arising from the use of point-group symmetry depend on the number of pairs of symmetry orbital sets for each irreducible representation (irrep), as arises in the supermatrix definition.[7] If there are n_A atoms, none of which are located on symmetry elements, and each has a basis set of n_F functions, then the AO representation consists of m ($=n_A n_F$) regular representations,[12] and the total number of basis functions is n ($=gm$), where g is the order of the group. A regular representation contains each irrep (λ) a number of times equal to its dimension (d_λ).[12] Assuming that m is a large enough number that only its leading power need be kept, the total number of pairs of symmetry orbital sets from the same irreps are

$$\sum_\lambda (md_\lambda)(md_\lambda)/2 = (m^2/2)\sum_\lambda d_\lambda^2 = m^2 g/2$$

and the total number of supermatrix elements is

$$(m^2g/2)(m^2g/2)/2 = m^4g^2/8 = (n^4/8)/g^2$$

Since $(n^4/8)$ is the total number of AO integrals, the overall reduction factor is g^2. Further analysis shows that approximately $(n^4/8)/g$ AO integrals are independent and need to be computed but that only $(n^4/8)/g^2$ linear (supermatrix) combinations of these integrals need to be used in SCF calculations.

Registry No. Be, 7440-41-7; Be_{69}, 127685-42-1.

(12) Slater, J. C. *Quantum Theory of Molecules and Solids*; McGraw-Hill: New York, 1963; Vol. 1.

Rotational Spectrum and Structure of the HCN-$(CO_2)_2$ Trimer

H. S. Gutowsky,* Jane Chen, P. J. Hajduk, and R. S. Ruoff

Noyes Chemical Laboratory, University of Illinois, Urbana, Illinois 61801 *(Received: November 10, 1989)*

Rotational spectra have been observed and rotational constants determined for HCN-$(CO_2)_2$, $H^{13}CN$-$(CO_2)_2$, $HC^{15}N$-$(CO_2)_2$, and HCN-$^{13}CO_2CO_2$ by using the Fourier transform, Flygare/Balle Mark II spectrometer with a pulsed nozzle. Less extensive observations were made of DCN-$(CO_2)_2$, HCN-$(^{13}CO_2)_2$, and two ^{18}O-substituted isotopic species. The rotational constants found for the parent asymmetric top are 1852.844, 1446.159, and 981.48 MHz for A, B, and C and -0.1085, -0.0297, -0.0241, -0.0190, and -0.0066 MHz for τ_1, τ_2, τ_{aaaa}, τ_{bbbb}, and τ_{cccc}, respectively. The isotopic substitution reveals a ground-state geometry with the C_2 symmetry of the slipped parallel $(CO_2)_2$ subunit and having the HCN along the C_2 axis, the N end closest to the $(CO_2)_2$. The C_2 symmetry is confirmed by the absence of *eo* and *oe* states as predicted for 2-fold symmetry with only equivalent bosons off-axis. The two carbons of the $(CO_2)_2$ lie in a plane R = 3.098 Å below the center of mass of the HCN. The C-C distance in this subunit is 3.522 Å, which is 0.077 Å shorter than reported for the free $(CO_2)_2$ dimer. Also, an inertial analysis shows the individual CO_2's to be counterrotated by γ = 20.3° out of the *ac* plane containing the carbons, the inner oxygens rotated away from the HCN. The OCC "slip" angle β is 60.8° in the $(CO_2)_2$. The torsional oscillations of the HCN are anisotropic, with an average displacement of 12.4°, as determined from isotopic substitution and the ^{14}N hyperfine structure (hfs). Virtually all of the hf components are doublets separated by 10-200 kHz. We attribute the doubling to an inversion of the clusters by a 140° counterrotation of the CO_2's. The inversion does not affect the dipole moment of the cluster, so the observed doubling is the difference in tunneling splittings of the rotational states for each transition.

Introduction

In a previous account[1] we described the rotational spectrum and structure of the HCN-$(CO_2)_3$ cluster. The present report is a companion study made of the HCN-$(CO_2)_2$ heterotrimer. Both clusters are formed by the addition of an HCN to a nonpolar homocluster of CO_2, the $(CO_2)_3$ cyclic trimer having a planar pinwheel geometry with C_{3h} symmetry[2] and the planar $(CO_2)_2$ dimer a slipped parallel structure[3] (Figure 1). In both cases the

(1) Gutowsky, H. S.; Hajduk, P. J.; Chuang, C.; Ruoff, R. S. *J. Chem. Phys.* **1990**, *92*, 862.

(2) Fraser, G. T.; Pine, A. S.; Lafferty, W. J.; Miller, R. E. *J. Chem. Phys.* **1987**, *87*, 1502.

0022-3654/90/2094-7774$02.50/0

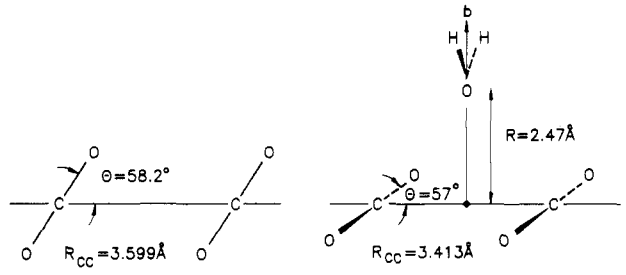

Figure 1. Structures reported previously for the planar, slipped parallel $(CO_2)_2$ dimer[3] (left) and the T-shaped H_2O–$(CO_2)_2$ trimer[4] (right).

HCN lies along the figure axis of the cluster with the nitrogen end closest to the carbons of the $(CO_2)_n$.

The geometry of the HCN–$(CO_2)_2$ trimer is similar to that reported recently[4] for H_2O–$(CO_2)_2$, also shown in Figure 1. They have a 2-fold axis of symmetry, and the C–C distance R_{CC} is reduced substantially from that in free $(CO_2)_2$. However, with HCN the CO_2's are rotated out-of-plane by repulsion between the inner oxygens and the nitrogen, as was reported for HC-N–$(CO_2)_3$.[1] In addition, the rotational transitions of the trimer are doubled at ~100 kHz by an ingenious type of quantum mechanical tunneling. Because of these interesting complexities in its structure, a number of isotopic species of the cluster were studied. The details are presented below, and the results are compared with those for H_2O–$(CO_2)_2$ and HCN–$(CO_2)_3$.

Experimental Section

The same pulsed nozzle, Fourier transform microwave spectrometer and experimental methods were used in the present work as for HCN–$(CO_2)_3$.[1] Here the best signal-to-noise ratio (S/N) was obtained with a mixture of about 0.1% HCN and 1% CO_2 in first-run neon (Airco, 70% Ne, 30% He), the CO_2 concentration about half the optimum for HCN–$(CO_2)_3$. The S/N for the strongest hyperfine components of the $1_{11} \rightarrow 2_{20}$ transition centered at 7236.663 MHz was about 5:1 for a single microwave pulse and 15:1 for the same transition of $HC^{15}N$–$(CO_2)_2$, which has no ^{14}N hyperfine structure (hfs).

$HC^{15}N$ and $H^{13}CN$ were prepared by adding orthophosphoric acid to $KC^{15}N$ and $K^{13}CN$ (Cambridge Isotope Laboratories), respectively. The $^{13}CO_2$ (99%) and CO_2 with 50% ^{18}O at random came from Cambridge Isotopes and the $C^{18}O_2$ (95%) from Isotec, Inc.

Results and Analysis

A. Identification, Hfs, and Rotational Constants. The HCN–$(CO_2)_2$ cluster was found while we were measuring transitions of $(HCN)_2$–CO_2.[5] A set of 10 fairly strong lines was observed at 7237 MHz, extending over 3 MHz. It looked very much like the ^{14}N quadrupolar hfs in a $J = 1 \rightarrow 2$ or $2 \rightarrow 3$ transition of a species with two $HC^{14}N$'s along a principal axis. The composition of the species was established by isotopic substitution. With the parent CO_2 replaced by 99% $^{13}CO_2$, the transition at 7237 MHz was replaced by a very similar one at 7175 MHz. Similarly, when the HCN was replaced by $HC^{15}N$, the 10-component transition at 7237 MHz was replaced by a doublet of ~100 kHz at 7184 MHz.

The number of CO_2 subunits was determined by searching between 7175 and 7237 MHz with a 50/50 mixture of $^{12}CO_2$ and $^{13}CO_2$. This turned up another set of 10 lines halfway between, at 7206 MHz, proving the cluster contains two CO_2's that are equivalent. A search of the 7184–7237 region with 50/50 $HC^{14}N$ and $HC^{15}N$ failed to uncover a transition, showing that the cluster contains only one HCN, making it an HCN–$(CO_2)_2$ trimer.

TABLE I: ^{14}N Hyperfine Structure[a] Fitted for Two Transitions of HCN–$(^{13}CO_2)_2$

comp F → F′	− state obsd, MHz	− state diff, kHz	+ state obsd, MHz	+ state diff, kHz	av obsd, MHz	av diff, kHz
			$1_{01} \rightarrow 2_{12}$ Transition			
1 → 2	4748.5367	−0.7	4748.5738	−0.6	4748.5553	−0.6
2 → 2	4749.1167	0.4	4749.1557	0.4	4749.1362	0.4
2 → 3	4749.7671	0.7	4749.8033	0.6	4749.7852	0.6
0 → 1	4750.9962	−0.5	4751.0340	−0.4	4751.0151	−0.4
			$1_{10} \rightarrow 2_{21}$ Transition			
1 → 2	6502.3660	−0.1	6502.4673	−0.6	6502.4167	−0.4
2 → 2	6502.9690	−0.1	6503.0716	0.5	6503.0203	0.0
1 → 1	6503.3377	−0.2	6503.4427	0.1	6503.3902	−0.1
2 → 3	6503.5940	0.5	6503.6978	−0.4	6503.6459	0.4
0 → 1	6504.8457	−0.1	6504.9507	0.3	6504.8982	0.0

[a] The χ_{gg} values obtained from the fit are given in Table II, and the line centers in Table V.

Moreover, with only one HCN per cluster the 10-component transitions must be caused by some type of inversion doubling by ~100 kHz of the five-line pattern for a single ^{14}N.

With the then known T-shaped HCN–CO_2 and planar, slipped parallel $(CO_2)_2$ dimers as models we thought it most likely for the trimer to be pseudo-T-shaped, consisting of the planar $(CO_2)_2$ dimer as a subgroup with the HCN along the C_2 symmetry axis of the group and the nitrogen end closest to and oscillating between the two carbons, similar to Ar_2–HF and –HCl.[6,7] If the geometry of the $(CO_2)_2$ dimer is unchanged by the interaction with HCN and if the N to CO_2 distance in the trimer is comparable with that in the T-shaped heterodimer, HCN–CO_2, the transition at 7237 MHz must be $1_{11} \rightarrow 2_{20}$. Only the *ee* and *oo* states and transitions between them are allowed for C_2 symmetry with only bosons off-axis.[8]

An initial estimate of the *A*, *B*, and *C* rotational constants was made by adjusting *R*, the HCN center of mass (cm) to $(CO_2)_2$ cm distance to fit the $1_{11} \rightarrow 2_{20}$ transition at 7237 MHz. This approach enabled us to find the same transition for the isotopic species DCN–$(CO_2)_2$ and $H^{13}CN$–$(CO_2)_2$ at 6995 and 7101 MHz, but it was unsuccessful at uncovering new transitions. We then learned of the work by Petersen[4] on the H_2O–$(CO_2)_2$ trimer in which the C–C separation was found to be 0.186 Å shorter than in free $(CO_2)_2$ dimer (Figure 1). Therefore, we made a new estimate of the rotational constants for the cluster by shrinking the C–C distance in the $(CO_2)_2$ by 0.1 Å and readjusting *R* to fit the $1_{11} \rightarrow 2_{20}$ transition at 7237 MHz.

This approach was successful in uncovering the $4_{04} \rightarrow 4_{13}$ and $2_{02} \rightarrow 3_{13}$ transitions, which were fitted along with the $1_{11} \rightarrow 2_{20}$ transition to obtain approximate *A*, *B*, and *C* values. These then enabled us to find other transitions, refine the rotational constants, and pinpoint the search, including that for a variety of isotopic species. In the course of the refinement it became necessary to obtain accurate line centers by fitting the hfs, which is affected by the tunneling doubling, by dependence of the ^{14}N quadrupole interaction constants χ_{aa} and χ_{cc} on the particular transition observed and by the anisotropy in χ_{gg}.

In the initial assignment and analysis of such cases it is useful[9] to reduce the complexity by choosing transitions for which the quadrupole interaction energies $E_Q(\kappa)$ are independent of Ray's asymmetry parameter $\kappa = (2B - A - C)/(A - C)$.[8] This became feasible when our studies were extended to clusters with the $(^{13}CO_2)_2$ species, for which the *eo* and *oe* states are allowed and the κ-independent $1_{10} \rightarrow 2_{21}$ and $1_{01} \rightarrow 2_{12}$ transitions were ob-

(3) Jucks, K. W.; Huang, Z. S.; Miller, R. E.; Fraser, G. T.; Pine, A. S.; Lafferty, W. J. *J. Chem. Phys.* **1988**, *88*, 2185. Walsh, M. A.; England, T. H.; Dyke, T. R.; Howard, B. J. *Chem. Phys. Lett.* **1987**, *142*, 265.

(4) Peterson, K. I.; Suenram, R. D.; Lovas, F. J. *J. Chem. Phys.* **1989**, *90*, 5964. We thank the authors for sending us a preprint.

(5) Ruoff, R. S.; Emilsson, T.; Chuang, C.; Klots, T. D.; Gutowsky, H. S. *J. Chem. Phys.* **1989**, *90*, 4069.

(6) Gutowsky, H. S.; Klots, T. D.; Chuang, C.; Schmuttenmaer, C. A.; Emilsson, T. *J. Chem. Phys.* **1987**, *86*, 569.

(7) Klots, T. D.; Chuang, C.; Ruoff, R. S.; Emilsson, T.; Gutowsky, H. S. *J. Chem. Phys.* **1987**, *86*, 5315.

(8) Gordy, W.; Cook, R. L. *Microwave Molecular Spectra*; Wiley: New York, 1984; pp 61, 661.

(9) Ruoff, R. S.; Emilsson, T. I.; Klots, T. D.; Chuang, C.; Gutowsky, H. S. *J. Chem. Phys.* **1988**, *88*, 1557.

TABLE II: ^{14}N Quadrupole Interaction Constants[a] Determined from the Hfs of the Two Tunneling States and from the Average Hfs for Transitions of HCN-$(CO_2)_2$ and HCN-$(^{13}CO_2)_2$

trans	state	χ_{aa}, MHz	χ_{bb}, MHz	χ_{cc}, MHz	η,[b] %
		HCN-$(CO_2)_2$			
$2_{02} \rightarrow 3_{13}$	−	1.941 (7)	−3.951	2.010	1.75
	+	1.945 (6)	−3.960	2.015	1.78
	av	1.943 (5)	−3.956	2.013	1.77
		HCN-$(^{13}CO_2)_2$			
$1_{01} \rightarrow 2_{12}$[c]	−	1.930 (4)	−3.953	2.023	2.36
	+	1.937 (4)	−3.951	2.014	1.95
	av	1.934 (3)	−3.952	2.018	2.15
$1_{10} \rightarrow 2_{21}$[c]	−	1.943 (1)	−3.954	2.011	1.74
	+	1.949 (1)	−3.961	2.012	1.60
	av	1.945 (1)	−3.957	2.012	1.67
$2_{02} \rightarrow 3_{13}$[d]	−	1.926	−3.976	2.050	3.13
	+	1.953	−3.965	2.012	1.50
	av	1.939	−3.970	2.031	2.33

[a] The numbers in parentheses are the standard deviation from the fit. [b] $\eta = (\chi_{aa} - \chi_{cc})/\chi_{bb}$; the standard deviation for it is about 0.1. [c] The hfs of this transition and its fit are given in Table I. [d] No standard deviation is given because only three hf components were fitted.

TABLE III: Some of the ^{14}N Hyperfine Interaction Constants Determined from the Averaged Hfs of the Low-J Transitions for Various Isotopic Species of HCN-$(CO_2)_2$[a]

species	trans, MHz	χ_{aa}, MHz	χ_{bb}, MHz	χ_{cc}, MHz	η, %
HCN-$(CO_2)_2$	$2_{02} \rightarrow 3_{13}$	1.943	−3.956	2.013	1.77
H^{13}CN-$(CO_2)_2$	$1_{11} \rightarrow 2_{02}$[b]	1.946	−3.964	2.018	1.81
	$2_{02} \rightarrow 3_{13}$	1.925	−3.957	2.032	2.70
HCN-$(^{13}CO_2CO_2)$	$1_{10} \rightarrow 2_{21}$	1.938	−3.959	2.021	2.09
	$1_{11} \rightarrow 2_{02}$[b]	1.946	−3.946	2.000	1.37
	$2_{02} \rightarrow 3_{13}$	1.966	−3.978	2.012	1.15
HCN-$(^{13}CO_2)_2$	$1_{01} \rightarrow 2_{12}$	1.934	−3.952	2.018	2.15
	$1_{10} \rightarrow 2_{21}$	1.945	−3.957	2.012	1.67
	$1_{11} \rightarrow 2_{02}$	1.949	−3.947	1.998	1.25
	$2_{02} \rightarrow 3_{13}$	1.939	−3.970	2.031	2.33

[a] The standard deviation for χ_{gg} is about 0.005, and for η about 0.1. [b] This transition had no resolved tunneling doublets.

served. The hfs found for these two transitions is listed in Table I. The data are given for the low- and high-frequency components of the tunneling doublet, arbitrarily designated as − and +, as well as for their average. The hfs was fitted in the coupled basis:

$$F = J + I \quad (1)$$

with χ_{aa} and $(1/6^{1/2})(\chi_{bb} - \chi_{cc})$ as adjustable parameters. The treatment is analogous to that employed for the chlorine hfs in the Ar_2–HCl asymmetric top.[7] The residues of fitting the four or five hf components are <1 kHz for all three data sets.

The χ_{gg} found by fitting these two transitions for HCN-$(^{13}C$-$O_2)_2$ and the $2_{02} \rightarrow 3_{13}$ transitions of HCN-$(^{13}CO_2)_2$ and HC-N-$(CO_2)_2$ are summarized in Table II for the − and + states as well as for the average hfs. It is seen that the magnitude of χ_{bb}, the principal component of the tensor, varies by about 0.5% while the perpendicular elements differ by up to 2%. In other words, the differences are primarily in the anisotropy of χ_{gg}:

$$\eta = (\chi_{aa} - \chi_{cc})/\chi_{bb} \quad (2)$$

which we use for descriptive purposes. The values given in the table for η show that the anisotropy tends to be higher in the − than in the + tunneling state. Moreover, the anisotropy depends somewhat on the transition observed as well as on the isotopic species.

With these results as a guide, the hfs was fitted for the various transitions and isotopic species. Typical values are given in Table III for the χ_{gg} obtained by fitting the averaged hfs. The line centers of the transitions were also obtained in an iterative fitting process that included provisional rotational constants. In most instances the line centers were obtained by fitting the hfs averaged for the − and + tunneling states. The results are given in Table IV for the parent species and in Table V for the other isotopic species. The separations of the tunneling doublets ν_d are also listed in Table IV for HCN-$(CO_2)_2$ and in Table VI for the other non-^{18}O isotopic species.

TABLE IV: Transitions and Separations of the − and + Tunneling Doublets Observed for HCN-$(CO_2)_2$[a]

trans	freq,[b] MHz	ν_d, kHz	diff (−), kHz	diff (+), kHz	diff (av), kHz
$1_{11} \rightarrow 2_{20}$	7236.663	135	5	5	5
$2_{02} \rightarrow 3_{13}$	6637.550	31	0	0	0
$4_{04} \rightarrow 4_{13}$	4173.656	162	19	21	20
$3_{22} \rightarrow 4_{31}$	13820.713	198	19	19	19
$3_{31} \rightarrow 4_{40}$	14276.647	211	−26	−25	−26
$5_{15} \rightarrow 5_{24}$	5664.582	195	−25	−27	−26
$5_{33} \rightarrow 5_{42}$	4450.286	120	−28	−30	−29
$5_{42} \rightarrow 5_{51}$	5298.414	190	13	13	13
$4_{22} \rightarrow 5_{33}$	14135.261	107	22	21	21
$4_{31} \rightarrow 5_{42}$	16385.944	171	1	4	3
$4_{40} \rightarrow 5_{51}$	17911.145	217	−20	−23	−21
$6_{15} \rightarrow 6_{24}$	5223.454	160	22	23	23
$6_{42} \rightarrow 6_{51}$	4616.188	106	21	23	22
rms dev of fit, kHz			19	20	20

[a] Residues, obsd − calcd, are given for fitting the line centers of the − and + components separately and for fitting their averages. The results of the fitting are given in Table VII. [b] The average of the line centers for − and + components.

TABLE V: Line Centers in MHz Determined by Averaging and Fitting the Hfs Observed for the − and + Components of Several Isotopic Species of HCN-$(CO_2)_2$

trans	DCN-$(CO_2)_2$[a]	H^{13}CN-$(CO_2)_2$[a]	HC^{15}N-$(CO_2)_2$[a]	HCN-$^{13}CO_2CO_2$	HCN-$(^{13}CO_2)_2$
$1_{11} \rightarrow 2_{02}$	4200.70	4209.134	4214.334	4176.125	4136.500
$1_{01} \rightarrow 2_{12}$					4749.544
$1_{10} \rightarrow 2_{21}$				6521.845	6503.406
$1_{11} \rightarrow 2_{20}$	6994.72	7101.581	7184.343	7205.746	7174.780
$2_{02} \rightarrow 3_{13}$	6407.505	6510.926	6589.457	6599.916	6562.262
$4_{04} \rightarrow 4_{13}$		4221.154	4192.897		
$3_{21} \rightarrow 4_{32}$				12371.027	
$3_{22} \rightarrow 4_{31}$		13673.117	13761.391	13739.944	
$3_{30} \rightarrow 4_{41}$				14133.468	
$3_{31} \rightarrow 4_{40}$		13904.808	14133.285	14236.163	
$5_{24} \rightarrow 5_{33}$			4569.33		
$5_{33} \rightarrow 5_{42}$		4160.915			
$4_{22} \rightarrow 5_{33}$		13739.034	13984.022	14091.577	
$4_{31} \rightarrow 5_{42}$		15913.963	16206.758		
$4_{40} \rightarrow 5_{51}$		17402.310	17716.411		
$6_{42} \rightarrow 6_{51}$			4376.477		
$5_{33} \rightarrow 6_{24}$		14276.277	14265.506		

[a] The even–odd and odd–even states are not allowed for this species.

TABLE VI: Tunneling Doublets in kHz Observed in Transitions of Several Isotopic Species of HCN-$(CO_2)_2$

trans	HCN-$(CO_2)_2$	DCN-$(CO_2)_2$	H^{13}CN-$(CO_2)_2$	HC^{15}N-$(CO_2)_2$	HCN-$^{13}CO_2CO_2$	HCN-$(^{13}CO_2)_2$
$1_{11} \rightarrow 2_{02}$		<15	<10	12	<10	<10
$1_{01} \rightarrow 2_{12}$						37
$1_{10} \rightarrow 2_{21}$					106	103
$1_{11} \rightarrow 2_{20}$	135	117	128	128	132	131
$2_{02} \rightarrow 3_{13}$	31	33	36	29	35	35
$4_{04} \rightarrow 4_{13}$	162		169	158		
$3_{21} \rightarrow 4_{32}$					148	
$3_{22} \rightarrow 4_{31}$	198		170	186	186	
$3_{30} \rightarrow 4_{41}$					202	
$3_{31} \rightarrow 4_{40}$	211		196	199	201	
$5_{15} \rightarrow 5_{24}$	195					
$5_{24} \rightarrow 5_{33}$				127		
$5_{33} \rightarrow 5_{42}$	120		110			
$5_{42} \rightarrow 5_{51}$	190					
$4_{22} \rightarrow 5_{33}$	107		100	104	114	
$4_{31} \rightarrow 5_{42}$	171		159	163		
$4_{40} \rightarrow 5_{51}$	217		205	205		
$6_{15} \rightarrow 6_{24}$	160					
$6_{42} \rightarrow 6_{51}$	106			95		
$5_{33} \rightarrow 6_{24}$			93	91		

TABLE VII: Rotation and Distortion Constants in MHz Determined for HCN–$(CO_2)_2$ by Fitting the Observed Line Centers (Table IV)[a]

const	− component	+ component	av centers
A	1852.825 (8)	1852.863 (8)	1852.844 (8)
B	1446.148 (7)	1446.170 (7)	1446.159 (7)
C	981.484 (8)	981.486 (9)	981.485 (8)
τ_1	−0.1074 (15)	−0.1095 (16)	−0.1085 (16)
τ_2	−0.0294 (5)	−0.0299 (5)	−0.0297 (5)
τ_{aaaa}	−0.0236 (8)	−0.0246 (9)	−0.0241 (9)
τ_{bbbb}	−0.0187 (7)	−0.0193 (7)	−0.0190 (7)
τ_{cccc}	−0.0066 (9)	−0.0067 (10)	−0.0066 (10)

[a] The numbers in parentheses are 1 standard deviation from the fit.

The line centers of the − and + components for HCN–$(CO_2)_2$ were fitted separately by the Kirchhoff program CDANAL for a distortable asymmetric rotor.[10,11] The residues are substantial, the rms deviations of the three fits being 20 kHz. The program was used to obtain the determinable parameters, the A, B, C rotational constants, and the five independent, fourth-order centrifugal distortion constants.[10] The results, listed in Table VII, show that the − state is slightly more compact and less distortable than the + state. However, the differences are well within the standard deviation for the fit; therefore, for the other isotopic species we present in Table VIII the constants found by fitting the average line centers. For the DCN–$(CO_2)_2$ and HCN–$(^{13}CO_2)_2$ isotopic species the centrifugal distortion constants were not determined. The fit for $HC^{15}N$–$(CO_2)_2$ is significantly better than for $H^{13}CN$–$(CO_2)_2$ and HCN–$^{13}CO_2CO_2$, probably because of inaccuracies in determining the line centers for the species with ^{14}N hfs.

B. Structural Analysis. Cluster Symmetry and Substitution Position of HCN. The symmetry of the cluster is given by the effects of the nuclear spins[12] in the isotopic species studied. Only transitions between *ee* and *oo* rotational states were found for clusters with only spin-zero nuclei (^{12}C and ^{16}O) in the $(CO_2)_2$ subunit. However, transitions between *eo* and *oe* states were observed in addition for clusters with either one or two spin-$^1/_2$ ^{13}C's in the CO_2's (Table V). But substitution of D, ^{13}C, and ^{15}N in the HCN did not affect the states and transitions allowed. So the cluster has a 2-fold axis with the HCN along it and the carbons of the CO_2's symmetrically off-axis. Inspection of the rotational constants (Tables VII and VIII) shows that B is virtually the same for the four HCN species, so the HCN lies along the b inertial axis. The orientation of the HCN with the N closest to the $(CO_2)_2$ is evident in the systematic increase in A and C with DCN, $H^{13}CN$, and $HC^{15}N$ substitution (Table VIII).

The rotational constants for these species, along with those for the ^{14}N parent, enable us to determine a substitution structure for the HCN in the cluster. For an asymmetric top with a 2-fold axis, atomic positions b_i along that axis are given in terms of the planar moments by[8]

$$\Delta P_b = \mu_s b_i^2 \tag{3}$$

where

$$\Delta P_b = \tfrac{1}{2}(-\Delta I_b + \Delta I_a + \Delta I_c) \tag{4}$$

and μ_s is the reduced mass of the substitution. Also, $\Delta I_b = I_b' - I_b$, where I_b is given by $I_bB = 505\,379.07$ μÅ^2 MHz. The b_i positions are referred to the center of mass of the parent cluster. They are averaged over the zero-point vibrations which are assumed to be unchanged by the substitution. For HCN, the vibrations are largely the torsional oscillations of the relatively rigid monomer about its cm, and the positions are its projections on the b axis for the average angular displacement.

The atomic positions and apparent bond distances determined in this manner for HCN are given in Table IX. The C–H distance is not reliable because deuterium substitution causes an appreciable change in torsional amplitude of the HCN. However, the C–N r_s distance of 1.1280 Å should be accurate. It is appreciably shorter than the 1.15512 Å found in the free monomer (Table X).

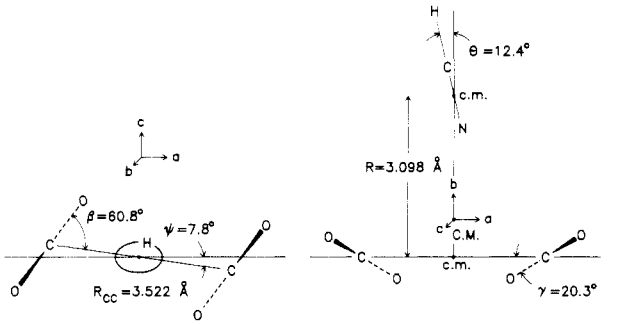

Figure 2. Top and side view planar projections of the asymmetric top structure determined in this study for the HCN–$(CO_2)_2$ cluster. The b axis is a 2-fold symmetry axis. The dashed lines in the CO_2's are to the inner oxygens, which are below the ac plane through the carbons, while the heavy solid lines are to the outer oxygens, which are above that plane.

Torsional Amplitude and χ_o of HCN. If χ_o^c, the ^{14}N hyperfine interaction constant in the rigid, equilibrium cluster were the same as χ_o^m, that in the free monomer, the observed projection of its principal component on the b axis of the cluster

$$\chi_b^c = \tfrac{1}{2}\langle 3\cos^2\theta - 1\rangle\chi_o^m \tag{5}$$

could be used to determine θ, the average torsional amplitude of the HCN. This approach, with −3.96 MHz for χ_b^c (Table III) and −4.708 MHz for χ_o^m (Table IX), gives a value of 19° for θ. However, cluster formation changes significantly the electric field gradient at the ^{14}N.[13] Therefore, we use the projection of the substitution C–N distance to find θ:[13,14]

$$r_s^c(\text{C–N}) = r_s^m(\text{C–N})\langle\cos\theta\rangle \tag{6}$$

where r_s^c(C–N) is the projection found in the cluster and r_s^m(C–N) is the bond distance in free HCN. The values of 1.1280 and 1.155 12 Å for these distances give θ to be 12.44°.

This substitution value for θ can now be used in eq 5 to estimate the extent by which cluster formation changes χ_o^m. We find χ_o^c to be −4.256 MHz, a 10% reduction from the monomer. For the HCN–$(CO_2)_3$ tetramer a similar analysis gave a 13% reduction.[1]

With a value in hand for χ_o^c, we can now analyze the anisotropy in the torsional vibration of the HCN. The procedure is the same as that employed for the HCl in the T-shaped acetylene–HCl dimer.[15] For the present inertial axis system the average angular displacements of the HCN from the b axis in the ba and bc planes are given respectively by

$$\cos\theta_{ba} = \left[\frac{\chi_{bb} + (\chi_o/2)}{\chi_{bb} + \chi_{aa} + \chi_o}\right]^{1/2} \tag{7a}$$

$$\cos\theta_{bc} = \left[\frac{\chi_{bb} + (\chi_o/2)}{\chi_{bb} + \chi_{cc} + \chi_o}\right]^{1/2} \tag{7b}$$

The extent of the anisotropy varies somewhat for different species and transitions (Table III). A typical case is the $1_{01} \rightarrow 2_{12}$ transition of HCN–$(^{13}CO_2)_2$, with $\eta = 2.15\%$. For it, θ_{ba} is found to be 10.0° and θ_{bc} to be 7.5°, which corresponds to $\theta = 12.44°$ by the relation $\tan^2\theta = \tan^2\theta_{ba} + \tan^2\theta_{bc}$.

Determination of R_{CC} and R. The size of the cluster is described largely by R_{CC}, the C–C distance in the $(CO_2)_2$ subunit, and by R, the HCN cm to $(CO_2)_2$ cm distance, both of which are readily

(10) Watson, J. K. G. *J. Chem. Phys.* **1967**, *46*, 1935.
(11) Kirchhoff, W. H. *J. Mol. Spectrosc.* **1972**, *41*, 333.
(12) Townes, C. H.; Schawlow, A. L. *Microwave Spectroscopy*; McGraw-Hill: New York, 1955.
(13) Ruoff, R. S.; Emilsson, T.; Chuang, C.; Klots, T. D.; Gutowsky, H. S. *Chem. Phys. Lett.* **1987**, *138*, 553.
(14) Goodwin, E. J.; Legon, A. C. *Chem. Phys.* **1984**, *87*, 81; *J. Chem. Phys.* **1985**, *82*, 4434.
(15) Legon, A. C.; Aldrich, P. D.; Flygare, W. H. *J. Chem. Phys.* **1981**, *75*, 625.

TABLE VIII: Rotation and Distortion Constants in MHz Determined for Several Isotopic Species of HCN-$(CO_2)_2$ by Fitting the Averages of the Line Centers for the - and + Tunneling Components (Table V)[a]

const	DCN-$(CO_2)_2$	$H^{13}CN$-$(CO_2)_2$	$HC^{15}N$-$(CO_2)_2$	HCN-$^{13}CO_2CO_2$	HCN-$(^{13}CO_2)_2$
A	1751.36	1797.274 (7)	1831.5329 (8)	1849.106 (5)	1845.07
B	1447.02	1446.362 (6)	1446.2545 (6)	1433.618 (8)	1421.21
C	952.32	965.616 (8)	975.5338 (7)	974.835 (6)	968.14
τ_1		-0.1073 (14)	-0.1024 (1)	-0.1046 (10)	
τ_2		-0.0287 (5)	-0.0277 (0)	-0.0280 (8)	
τ_{aaaa}		-0.0238 (7)	-0.0242 (1)	-0.0251 (7)	
τ_{bbbb}		-0.0170 (12)	-0.0173 (1)	-0.0155 (35)	
τ_{cccc}		-0.0031 (16)	-0.0043 (1)	-0.0057 (23)	
rms dev, kHz	dna[b]	10	1.6	5	dna[b]

[a] The entries in the table were determined from 3-, 11-, 12-, 9-, and 5-line centers, respectively. [b] Does not apply.

TABLE IX: Spectroscopic and Structural Properties[a] of Free HCN, CO_2, and $(CO_2)_2$

HCN[b]		CO_2[c]		$(CO_2)_2$[d]	
property	value	property	value	property	value
B_0	44315.9757	B_0	11698.2	R_{CC}	3.599
r_s(H-C)	1.06317	r_0(C=O)	1.16208	β, deg	58.2
r_s(C-N)	1.15512				
$\chi_0(^{14}N)$	-4.7079				

[a] Spectroscopic properties are in MHz and distances in angstroms. [b] References 17 and 18. [c] Reference 2. [d] Reference 3.

TABLE X: Substitution Structure Obtained from Four Isotopic Species of HCN-$(CO_2)_2$ Compared with the Parameters from Fitting the Moments of Inertia Observed for the Same Isotopomers[a]

atom	coord	value, Å	property	value, Å, deg	param	subst, Å, deg	inertial, Å, deg
H	b	3.9913	r_s(H-C)	1.0728	R_{cm}	3.0977	3.0943
C	b	2.9185	r_s(C-N)	1.1280	R_{CC}	3.4949	3.5223
N	b	1.7905	θ	12.44	$\beta(CO_2)$	60.3	60.8
	a	1.7334	θ_{ba}	10.03	$\gamma(CO_2)$	15.5	20.3
C	b	0.7252	θ_{bc}	7.52	$\psi(CO_2)$	7.3	7.8
	c	0.2212					

[a] The fit incorporated the substitution results for the torsional vibrations of the HCN.

determined by a substitution analysis. For this purpose we used planar moment expressions for an asymmetric top,[8] similar to eqs 3 and 4. They give the coordinates of the ^{13}C in the inertial frame of the parent HCN-$(CO_2)_2$ with the cm of the cluster as origin. The rotational constants in Tables VII and VIII lead to values for a_i, b_i, and c_i of 1.7334, 0.7252, and 0.2212 Å, respectively, corresponding to the basic structure shown in Figure 2. Because of symmetry the two carbons of $(CO_2)_2$ are in an ac plane through the cm of the subunit. Thus, R_{CC} is $2(a_i^2 + c_i^2)^{1/2}$ or 3.4949 Å. A similar analysis of the approximate rotational constants found for the di-^{13}C-substituted species gave results agreeing within a few thousandths of an angstrom with those for mono-^{13}C substitution.

We see that the cm of the $(CO_2)_2$ is 0.7252 Å "below" the cm of the cluster. The substitution positions along the b axis previously determined for the C and N of HCN correspond to its cm being 2.3725 Å "above" the cm of the cluster. Their sum of 3.0977 Å is R.

Angular Structure of the $(CO_2)_2$. For the $(CO_2)_2$ dimer the planar, slipped parallel structure was found[3] to have an angle (β) of 58.2° between the inner CO_2 axes and the C-C axis (Figure 1). Also, in the HCN-$(CO_2)_3$ cluster the CO_2's were found to be rotated out of plane by an angle (γ) of 36.9°, with the inner oxygen away from the HCN. In the present cluster a value for γ can be readily determined from I_b and the results given above for R_{CC} and θ. Application of the parallel axis theorem[16] to the clusters taken to be rigid except for the HCN torsion shows that for the clusters with 2-fold symmetry

$$I_b = \tfrac{1}{2}m(CO_2)R_{CC}^2 + I(HCN)\sin^2\theta + 2I(CO_2)\cos^2\gamma \quad (8)$$

where $m(CO_2)$ is the mass of the CO_2 and I(HCN) and $I(CO_2)$ are the moments of inertia for the free monomers (Table IX).[2,17,18] Solving this equation gives γ to be 15.44° in the parent species, HCN-$(CO_2)_2$, and 15.52° and 15.49° in the $H^{13}CN$ and $HC^{15}N$ isotopomers. The C_2 symmetry of the clusters requires that the two CO_2's be counterrotated; however, eq 8 does not tell whether the inner or outer oxygens are rotated away from the HCN.

The determination of β is a bit more complicated. Analytical expressions derived[16] for I_a and I_c in the isotopomers with a 2-fold axis show that β affects both of them and can be found from either in a manner similar to that for γ. However, the planar moment

$$P_a = \tfrac{1}{2}(-I_a + I_b + I_c) \quad (9)$$

combines both dependences in the simpler expression

$$P_a = 2m(CO_2)a_C^2 + \tfrac{1}{2}I(HCN)\sin^2\theta_{ba} + 2I(CO_2)\sin^2\alpha \quad (10)$$

where a_C is the distance along the a axis of the CO_2 cm from the $(CO_2)_2$ cm and α is the angle in the ac plane between the c axis and the projections of the CO_2 axes.

In turn, β is given by

$$\beta = 90° - \alpha + \psi \quad (11)$$

where ψ is a dependent parameter, the angle between the a axis and the C-C axis. Application of this approach to the rotational constants of the four species with a 2-fold axis gives an average for β of 60.3°, with a very narrow range in values of only 0.03°.

Inertial Analysis. The substitution structure is summarized in Table X. The model employed for its determination neglects all vibrations except for the torsional oscillations of the HCN. Even so, an overall substitution structure usually fits fairly well the moments of inertia observed for a small cluster for the isotopic species employed in the substitution analysis. At least this was so for the HCN-$(CO_2)_3$ symmetric tops.[1] However, in the present case the substitution structure predicts rotational constants for the four isotopic species employed that are about 10 MHz larger than observed for both A and C but with an rms deviation of only 150 kHz for B. Another view of this discrepancy is seen by using a computer program to fit the rotational constants found for the isotopomers HCN-$(CO_2)_2$, $H^{13}CN$-$(CO_2)_2$, $HC^{15}N$-$(CO_2)_2$, and HCN-$(^{13}CO_2CO_2)$.

In the program, the HCN and CO_2 molecules were assumed to have the structures of the free monomers (Table IX). R_{CC}, R, β, and γ were used as adjustable parameters, but C_2 symmetry was imposed on them. The effects of the anisotropic torsional oscillations of the HCN were included but held constant. The results of the fit are listed in Table X. The same fit was obtained by rotating the inner oxygen of the CO_2's either away from or toward the nitrogen ($\pm\gamma$). Also, the best-fit parameters are little affected by exclusion of the rotational constants for the non-C_2 species HCN-$(^{13}CO_2CO_2)$ in the fit. Comparison of the substitution and inertial results shows that they are about the same for R_{cm} and β but that the inertial values of R_{CC} and γ are

(16) Symon, K. R. *Mechanics*; Addison-Wesley: Reading, MA, 1971; p 225.

(17) Delucia, F.; Gordy, W. *Phys. Rev.* **1969**, *187*, 58.

(18) Pearson, E. F.; Creswell, R. A.; Winnewisser, M.; Winnewisser, G. *Z. Naturforsch.* **1976**, *31a*, 1394.

TABLE XI: Effects of ^{18}O Substitution on Transition Frequencies, Hfs, and Tunneling Doublets of the HCN–$(CO_2)_2$ Trimer

trans	obsd, MHz	predicted,[a] MHz	χ_{bb},[b] MHz	η, %	ν_d, kHz
		HCN–(^{18}OCOCO$_2$)[c]			
$2_{02} \rightarrow 3_{13}$	6564.92	6562.54	−3.958	1.09	≲10
$1_{11} \rightarrow 2_{20}$	7117.44	7116.57			48
		HCN–(C^{18}O$_2$CO$_2$)			
$2_{02} \rightarrow 3_{13}$	6453.35	6449.86	−3.919	3.06	29
$1_{11} \rightarrow 2_{20}$	7019.55	7019.17			95

[a] The predicted transitions are for the inner oxygens rotated away from the HCN. [b] The two transitions were fitted jointly for each species. [c] The ^{18}O is in an inner position.

significantly larger, 3.522 versus 3.495 Å and 20.3° versus 15.5°. The net effect is that the structure obtained by fitting the rotational constants has a less compact $(CO_2)_2$ subunit. The need to rotate the CO_2's out-of-plane was verified by fitting the rotational constants for the four isotopic species with the constraint that $\gamma = 0$. In this case the rms deviation of the fit was an order of magnitude larger, 0.6 versus 0.07 MHz.

Effects of ^{18}O Substitution. The sign of γ was established as positive by observing the $1_{11} \rightarrow 2_{20}$ and $2_{02} \rightarrow 3_{13}$ transitions of the mono-inner ^{18}O-substituted species, HCN–(^{18}OCOCO$_2$), and an inner and outer ^{18}O-disubstituted species, HCN–(C^{18}O$_2$CO$_2$). The substitution results for the HCN torsion, the inertial values for the other structural parameters, and the centrifugal distortion of the parent were used to predict the spectra for the various ^{18}O-substituted species with γ both + and −. The observed line centers are compared in Table XI with those calculated for the inner oxygens rotated away from the HCN (+γ). It is seen that the observed frequencies are within 2 or 3 MHz of those calculated for +γ. Moreover, each of the frequencies calculated for these transitions with −γ differ by at least 10 MHz from those observed.

The hfs found for the mono-^{18}O species is similar to that for the other isotopic species (Table III). However, that for the di-^{18}O species shows the torsional oscillations of the HCN to be more anisotropic in it. Also, it is seen in Table XI that ^{18}O substitution has a much larger effect on the tunneling doublets than isotopic substitution for any of the other nuclear species (Table VI). A search was not made for other than *ee* ↔ *oo* transitions. A more detailed study of the numerous ^{18}O substituted species could aid in understanding the tunneling mechanism, but it is beyond the scope of our present work.

C. Inversion Doubling. The doubling of the transitions and their hfs is an interesting aspect of the results. It is exhibited by all of the numerous isotopic species examined (Tables VI and XI) and ranges from ≲10 kHz for $1_{11} \rightarrow 2_{02}$ transitions to 200 kHz for higher J. Substitution of heavier nuclei in the HCN or of the carbons in the CO_2's has little effect on the doublets, decreasing them by only 5–10% from the values in the parent species. On the other hand, ^{18}O substitution has more major effects. Oddly enough, mono-^{18}O substitution has a substantially larger effect than di-^{18}O substitution in a single CO_2. The doublet splittings in HCN–(^{18}OCOCO$_2$) are only a third of those in the parent while those for HCN–(C^{18}O$_2$CO$_2$) are larger but appreciably less than in the other isotopic species, at least for the $1_{11} \rightarrow 2_{20}$ transition (95 versus 117–135 kHz). In contrast, mono- and di-^{13}C substitution in the CO_2's has virtually no effect on the splittings. This indicates that the oxygens are the nuclei primarily involved in the tunneling.

The most likely cause of the doublets is an inversion corresponding to reflection of the cluster in the *bc* plane, a process that can occur for all isotopic species. It is accomplished readily by an ~140° counterrotation of the two CO_2's about the *a* axis, as shown in Figure 3. The direction of the rotation is such that the inner oxygens initially move away from the HCN. Tunneling through the barrier to this inversion splits each rotational level into states of − and + parity. However, there is no change in dipole moment associated with the inversion, so transitions between the − and + states are not observed. Instead, each rotational transition

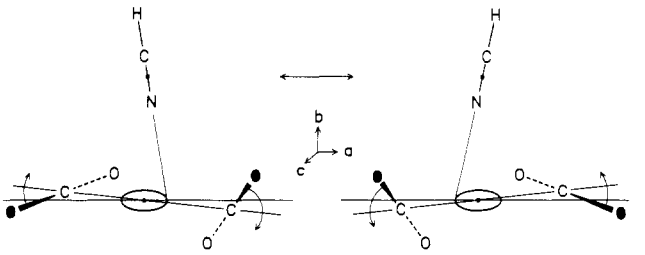

Figure 3. Model proposed for the tunneling inversion of the HCN–$(CO_2)_2$ trimers.

has two components, one for states of − parity and the other for the + states. The separation ν_d observed between them is simply the difference in tunneling splittings ν_t for the two rotational states, that is, $\nu_d = \nu_t' - \nu_t$. In turn, the differences in ν_d for different transitions are attributable to centrifugal distortion, an interpretation consistent with the much closer doublets found for small J.

Discussion

Our results for the HCN–$(CO_2)_2$ trimer provide some interesting similarities to the HCN–$(CO_2)_3$ tetramer and some interesting differences. In both clusters the CO_2's are rotated out of the plane,[19] with the inner oxygens away from the HCN. Moreover, the interactions with the HCN serve to contract the $(CO_2)_n$ subunits appreciably. The contraction of the $(CO_2)_2$ dimer and the CO_2 out-of-plane rotation in it are less than found in the HCN–$(CO_2)_3$ cluster, suggesting that the latter is more tightly bound. This view is supported by the smaller perturbation of the ^{14}N electric field gradient in the smaller cluster and by the larger cm (HCN) to C distance, 3.703 Å in the trimer versus 3.525 Å in the tetramer.[1]

The slip-parallel displacement, on the other hand, seems to be relatively insensitive to cluster formation by the $(CO_2)_2$ dimer. The inner OCC angle β is reported to be 58.2° in the dimer[3] and 57° in the H_2O–$(CO_2)_2$ trimer.[4] We find it to be 60.8° in the HCN–$(CO_2)_2$ cluster, which gives a small range of 4° for three quite different isotopic species.

The differences between the substitution values of R_{CC} and γ and those from fitting the rotational constants call for attention. They probably arise from the large amplitude torsional oscillation of the CO_2's associated with the inversion and the inaccessibility of its major effects. The inversion frequencies themselves are probably several orders of magnitude larger than the differences in them between states of opposite parity, which is all we observe. The substitution analysis assumes that the structure is not perturbed by the substitution, but it is, as is the tunneling. No doubt the perturbation is less for substitution in the HCN than in the $(CO_2)_2$ subunit. Therefore, we consider the HCN substitution results to be reliable for θ and R_{cm} but prefer the inertial results for R_{CC}, β, and γ. It is to be noted, however, that this preference is somewhat arbitrary in view of the highly floppy nature of the cluster.[20]

The large difference between the out-of-plane rotation of 37° in HCN–$(CO_2)_3$ compared to 20.3° for HCN–$(CO_2)_2$ implies that the dependence on γ of the potential function has a relatively broad and shallow minimum. This is apparent also in the observed inversion, which seems to be primarily a rotation of the two CO_2's through a large excursion in γ (Figure 3). Another aspect of the potential function is shown by the anisotropy in the torsional vibration of the HCN. The HCN can oscillate more readily along the C–C axis of the $(CO_2)_2$ subunit (θ_{ba}) than perpendicular to the axis (θ_{bc}). This was also found to be the case for the T-shaped Ar_2–HX (X = F and Cl) trimers.[6,7]

The nature of the tunneling mechanism requires more detailed exploration. The possible pathways interconverting isomeric forms

(19) A further analysis of H_2O–$(CO_2)_2$ suggests that in it the CO_2's are also rotated out-of-plane. Gutowsky, H. S.; Chuang, C. *J. Chem. Phys.*, in press.

(20) Nesbitt, D. J.; Naaman, R. *J. Chem. Phys.* **1989**, *91*, 3801.

of the trimer are complex, involving both translation and rotation of the CO_2's. Three types of pathway can be distinguished: (1) the translation of both CO_2's parallel to and toward one another along the slip axis, accompanied by counterrotation of the CO_2's through 2γ about the C–C axis to interchange the inner and outer oxygens; (2) a windshield wiper rotation of the CO_2's about the *b* axis, also accompanied by counterrotation about the C–C axis; (3) an "out-of-plane" rotation of the CO_2's through an angle of $(180° - 2\gamma)$ as shown in Figure 3. In all types of inversion the HCN is largely a spectator, experiencing only minor adjustments in its vibrational orientation without generating a net dipole in the *ac* plane.

Of these pathways (1) and (2) are discounted because of probably large barriers. For (1) an electrostatic calculation by Howard[3] of the potential of the $(CO_2)_2$ dimer as a function of a slip-distance parameter gave a very large barrier of 1100 cm^{-1}. Pathway (2) is similar to (1) but has a somewhat smaller barrier. Further evidence for the stiffness of the slip parallel displacement is provided by the insensitivity of β to cluster formation of the $(CO_2)_2$ with HCN and H_2O. Another argument against pathways (1) and (2) is that they interchange inner and outer oxygens. For them, the tunneling found in the mono-^{18}O species would involve two distinguishable isomers. This need not quench tunneling if its frequency in the homonuclear case is larger than the zero-point energy difference between the two different isomers. For example, tunneling has been reported[21] for the heterodimer $H^{35}Cl$–$H^{37}Cl$. But the necessary conditions seem unlikely to be met in the present case. A final argument against (1) is that it requires both carbons in the CO_2's to move as much as the oxygens but ^{13}C substitution in one or both CO_2's is virtually without effect on ν_d compared to ^{18}O substitution.

With type (3) pathways, it seems most likely that the CO_2's would rotate so that the inner oxygens move further away from the nitrogen. The resulting counterrotation could also preserve the center of mass. However, the rotations could either preserve or interchange inner and outer oxygens depending upon which axes of rotation are favored by the potential surface. Rotation of the CO_2's about axes effectively parallel to the *a* axis (Figure 2) would preserve the oxygen sets, while rotation about axes in the *ac* plane containing the carbons, perpendicular to the CO_2's, would interchange the oxygen sets. Of these two options the former seems preferable for the reasons given in the preceding paragraph.

This pathway is shown schematically in Figure 3. It accounts for the small effect of D, ^{13}C, and ^{15}N substitution on ν_d and for the much larger effects of ^{18}O. Also, it is in accord with the various indications that the potential surface for CO_2 out-of-plane rotation has a relatively shallow minimum.

Acknowledgment. We thank Carl Chuang, Tryggvi Emilsson, and Tim Klots for their interest and help in this work, especially Carl Chuang for assistance with the data analysis. We are indebted to Professor D. H. Secrest for a critique of the tunneling mechanism. The research was supported by the National Science Foundation under Grants No. CHE 88-20359 and DMR 86-12860. Also, acknowledgment is made to the donors of the Petroleum Research Fund, administered by the American Chemical Society, for partial support of this research.

Registry No. HCN, 74-90-8; DCN, 3017-23-0; $H^{13}CN$, 20722-83-2; $HC^{15}N$, 13127-85-0; CO_2, 124-38-9; $^{13}CO_2$, 1111-72-4; $C^{18}O_2$, 18983-82-9; N_2, 7727-37-9.

(21) Ohashi, N.; Pine, A. S. *J. Chem. Phys.* **1984**, *81*, 73.

Theoretical Studies of Diphosphene and Diphosphinylidene. 2. Some Unusual Features of the Radical Cations and Anions

Thomas L. Allen,*[†] Andrew C. Scheiner,[‡,§] and Henry F. Schaefer III[‡,§]

Department of Chemistry, University of California, Davis, California 95616, Department of Chemistry, University of California, Berkeley, California 94720, and Center for Computational Quantum Chemistry,[∥] School of Chemical Sciences, University of Georgia, Athens, Georgia 30602 *(Received: November 21, 1989; In Final Form: March 6, 1990)*

Various states of $HPPH^+$ and H_2PP^+ cations have been studied by using ab initio molecular electronic structure theory. These include the ^2A_g, ^2A_u, and ^2B_u states of *trans*-$HPPH^+$, the $^2B_1$ and $^2A_1$ states of *cis*-$HPPH^+$, and the $^2B_2$ and $^2B_1$ states of planar H_2PP^+. The cationic state of lowest energy is the planar H_2PP^+ $^2B_2$ state. For *trans*-$HPPH^+$ the SCF results are misleading; they indicate that a skewed $HPPH^+$ ^2A state lies below the trans states. However, optimization at the CISD level of theory shows that the *trans*-$HPPH^+$ ^2A_g state is the most stable $HPPH^+$ cationic state. Four anionic states were studied by using an extended basis set with diffuse functions: *trans*-$HPPH^-$ ^2B_g, *cis*-$HPPH^-$ $^2A_2$, planar H_2PP^- $^2B_2$, and pyramidal H_2PP^- $^2A'$. The first of these has the lowest energy, but planar H_2PP has the highest electron affinity (to form the pyramidal anion). Finally, bond orders in the various states are analyzed.

Introduction

In a previous quantum mechanical study[1] of the various quantum states of diphosphene, HPPH, and its isomer diphosphinylidene (also called phosphinophosphinidene), H_2PP, we reported that the vertical ionization energies of *trans*-diphosphene showed a violation of Koopmans' theorem. An understanding of such violations is of course important in connection with experimental studies of cations and anions in mass spectrometry, etc. To obtain more information on this point, we have carried out a theoretical examination of the various cationic species with basis sets of high quality. For completeness we have also studied the anions. The results we present on the various states studied here should be useful as a guide to future experimentation on H_2P_2 and its radical cations and anions.

Diphosphene is the object of much current interest because it supposedly has the highly unusual feature of a phosphorus–

[†] University of California, Davis.
[‡] University of California, Berkeley.
[§] University of Georgia.
[∥] Contribution CCQC No. 75.

(1) Allen, T. L.; Scheiner, A. C.; Yamaguchi, Y.; Schaefer, H. F., III. *J. Am. Chem. Soc.* **1986**, *108*, 7579.

0022-3654/90/2094-7780$02.50/0